J. Membrane Biol. 53, 143–156 (1980)

The Journal of
Membrane Biology

Dual Effects of K Ions upon the Inactivation of the Anomalous Rectifier of the Tunicate Egg Cell Membrane

Harunori Ohmori*

Department of Physiology, Institute of Brain Research, School of Medicine, University of Tokyo, Tokyo, Japan

Summary. Inactivation of the K inward current through the anomalous rectifier channel of the egg cell membrane of a tunicate, *Halocynthia roretzi* Drashe, was studied under voltage-clamp. The noise spectrum of the steady-state current recorded at hyperpolarized potentials was measured in solutions in which Na, Cs, Hydrazine, or Sr caused inactivation of the current. The unitary conductance estimated was independent of which cation caused inactivation. From the relation between the concentration of cations which caused inactivation and the extent of inactivation at fixed potentials, the binding of one inactivator to a channel was found to cause inactivation, and the potency of inactivation was $Cs^+ > Hydrazine^+ > Na^+ > Li^+$, and $Ba^{2+} > Sr^{2+}$. The inactivation caused by Na^+ was increased by K^+ when $[K]_o$ was lower than 20 mM, but was decreased by K^+ in higher K-ASW (artificial sea water). One K^+ was found to inactivate the channel cooperatively with one Na^+. Increase of inactivation by K^+ was a dominant effect in Cs-ASW. The inactivation was explained quantitatively by a model assuming cooperative plugging by a monovalent inactivator and a K^+.

Key words: anomalous rectifier, inactivation, K inward current.

The inward K current through the anomalous rectifier in the cell membrane of starfish eggs and of frog skeletal muscle is inactivated in a solution containing small amounts of Cs or Ba ions (Hagiwara, Miyazaki & Rosenthal, 1976; Gay & Stanfield, 1977; Hagiwara et al., 1978; Standen & Stanfield, 1978). The inactivation of the K inward current through the anomalous rectifier in the egg cell membrane of the tunicate is caused by Na ions in the sea water (Ohmori, 1978). These observations suggest some interaction of ions other than K^+ with K channel.

The stoichiometric studies made above on the K inward currents either in the starfish egg membrane or in the frog skeletal muscle have shown that these cations bind one-to-one to the channel. However, the steep potential dependence of the inactivation could not be explained by the one-to-one binding of the monovalent cation to the channel (Hagiwara et al., 1976; Ohmori, 1978). Some cooperative interaction, either with a structure inherent to the channel or with some other cations, is expected for the inactivation caused by monovalent cation (Na or Cs). Hagiwara et al. (1976) reported that the blocking effect of Cs increases with $[K]_o$ compared at a fixed potential.

In the present experiments, the interactions between K channels for the inward rectification and some of the alkalimetal, alkaline earth, or organic cations are studied under voltage-clamp condition. The experimental results show that K^+ ions have dual effects on the inactivation; they may either increase (facilitate) or decrease (suppress) the inactivation, depending upon their concentration and membrane potential.

Material and Methods

Preparations

Unfertilized eggs of the tunicate, *Halocynthia roretzi* Drashe, were used. The preparation of eggs, the control of the bath temperature (15 °C), and the recording chamber were described in a previous paper (Ohmori, 1978).

* *Present address:* Dr. Harunori Ohmori, Division of Neurobiology & Behavior, College of Physicians & Surgeons, Columbia University, 630 West 168th Street, New York, New York 10032.

0022-2631/80/0053-0143 $02.80

Table 1. Solutions[a]

Type	Inactivator[b]	NaOH	Choline-Cl	KCl	KOH	$CaCl_2$	$MgCl_2$	Buffer
A	–	–	450	35	15	10	30	10-PIPES-K
B	400 Na	–	50	35	15	10	30	
C	1 Cs	–	450	35	15	10	30	
D	450 Hyd.[c]	–	–	35	15	10	30	
E	100 Sr	–	300	35	15	10	30	
F	1 Ba	–	450	35	15	10	30	
G	185 Na	15	–	300	–	10	30	10-PIPES-Na
H	185 Na	15	300	–	–	10	30	

[a] Concentrations in mM/liter. Inactivators are in chloride form.
[b] Inactivators.
[c] Hydrazine.

Solutions

Most solutions used are listed in Table 1. In the second column, labelled "Inactivator," the test cation is presented. Intermediate concentrations of test cations were obtained by mixing solution A with one of the other solutions (B to F). Small differences in the total ionic concentration of solutions C and F from the others caused no osmotic effects on the egg. The pH of the solution was adjusted to 7.0 by PIPES-K for A to F, and by PIPES-Na for G and H. In the Results section, these solutions are referred to as Na-ASW or Sr-ASW, adding the name of test cation before ASW. The KCl concentration in solution A, C, and E was changed by replacing it with choline-Cl in some experiments. In addition to the above eight solutions, Na-free, K-free ASW was used to detect nonspecific leakage current at the end of each experimental series. pH was adjusted to 7.0 by PIPES-TMA in this solution.

Data Recording and Processing

All the experiments were done under voltage-clamp with two glass micro-electrodes. A precise description of the voltage-clamp circuit was given in a previous paper (Okamoto, Takahashi & Yoshii, 1976).

The kinetics of the K inward current through the anomalous rectifier channel in Na-ASW has been described quantitatively in the previous paper (Ohmori, 1978). The inactivation parameters, s_∞ and τ_s were determined by a semilogarithmic plot of the transient component ($\Delta I(t) = I(t) - I_\infty$) of current against time, assuming no inactivation at the holding potential ($s_o = 1$). In this paper, the extent of inactivation was expressed as the ratio, $\Delta I/I_\infty$, where I_∞ is the steady-state current. The time-course of inactivation studied in the present work was much faster than that studied in the previous paper; therefore, the time interval between the beginning of potential step and the time at which the new potential level was reached was not negligible. ΔI was thus estimated as the value of the falling phase of $\Delta I(t)$ extrapolated to δt after the onset of voltage pulse, instead of to zero time. δt was about 1 msec and was determined by the method described previously (the constant time delay for the Na inward current; Okamoto et al., 1976; Keynes & Rojas, 1976).

The recording and filter systems and the data processing for the current noise were similar to those given in the previous paper (Ohmori, 1978). The steady-state current noise was fed to a 12 bits A/D converter, sampled uniformly at 10 or 5 msec intervals. When current noise was sampled at 5 msec intervals, the cutoff frequency of the low pass filters with 12 dB/octave roll-off was 200 Hz and that for the filters with 18 dB/octave roll-off was 160 Hz. These filters were used to prevent aliasing (Bendat & Piersol, 1971). Current noise spectra were displayed on a Tektronix oscilloscope (model 5010) in X–Y mode after about 25 sec processing time. After displaying, the spectral data was stored on a floppy disc and the next noise was sampled and analyzed. In this paper every steady-state current noise was analyzed on-line using PDP-11/03 LAB-System (DEC).

The cut-off frequency, the low frequency asymptotic value of the power density spectrum, unitary conductance, and the number of channels per egg were estimated from off-line displayings on a VT-55 graphic terminal (DEC). Curves were fitted by the least squares method to a series of data points within an appropriately confined region (from about 0.3 to about 45 Hz).

System Noise

Noise generated by the recording system and the resting membrane was assumed to be equal to that of the noise observed at zero-current condition. The power of electrical noise observed at zero-current condition (▲ in Fig. 1) was much smaller than the current noise observed at hyperpolarized membrane. Thus, the background noise was neglected and the test noise was analyzed without any background subtraction.

Results

Inactivation and Steady-state Current Noise of Anomalous Rectifier

As described previously (Ohmori, 1978), the anomalous or inward rectification was detected when the membrane was stepped from the holding (zero-current) potential to more negative potentials. The current is exclusively carried by K ions and showed membrane-potential-dependent inactivation in Na-ASW. The inactivation was, however, removed when the external Na was replaced with choline (Ohmori, 1978). When Cs^+, Hydrazine$^+$, Sr^{2+}, or Ba^{2+} was added to the Na-free ASW (Table 1) the inactivation reappeared. The inactivation time course in Cs^+, Hydrazine$^+$ or Sr^{2+} media was faster than that in Na medium (Fig. 1*B*, *C*, *D*, insets), whereas it was slower in Ba^{2+} medium (Fig. 1*A–b*). Similar time and potential dependent inactivation of the anomalous rectification current has been reported in the starfish egg

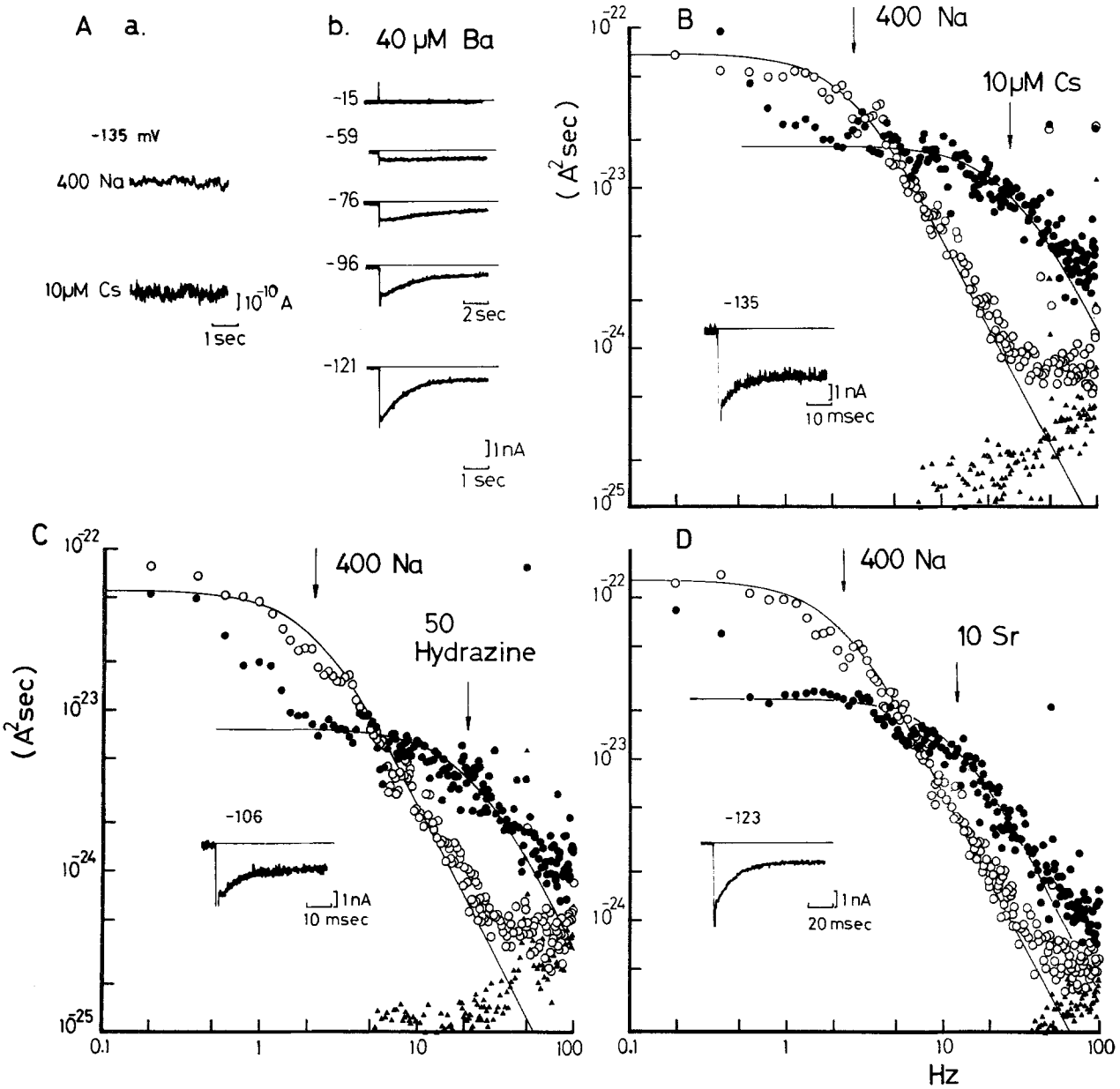

Fig. 1. Traces of inward K currents and the power density spectrum (pds.) of steady-state current noise. (*Aa*): The steady-state current noise; both recorded at −135 mV from the same cell; (*b*): the inactivation observed in Ba−ASW. (*B*) pds at −135 mV in 400 Na, 50 K−ASW ($I_\infty = -2.82$ nA, $f_c = 2.79$ Hz, $s_\infty = 0.65$, $\gamma = 6.6$ pmho, $N = 7{,}000$), in 10 μM Cs, 100 K ASW ($I_\infty = -3.3$ nA, $f_c = 31.98$ Hz, $s_\infty = 0.61$, $\gamma = 11.7$ pmho, $N = 4{,}100$) and the system noise (▲) recorded at −21 mV. (*C*): pds at −110 mV in 400 Na, 50 K−ASW ($I_\infty = -5.0$ nA, $f_c = 2.27$ Hz, $s_\infty = 0.78$, $\gamma = 5.21$ pmho, $N = 17{,}800$), in 50 Hydrazine, 50 K−ASW ($I_\infty = -1.82$ nA, $f_c = 21.61$ Hz, $s_\infty = 0.38$, $\gamma = 5.8$ pmho, $N = 12{,}000$), and the system noise at 0 mV. (*D*): pds at −121 mV in 400 Na, 50 K−ASW ($I_\infty = -4.9$ nA, $f_c = 2.32$ Hz, $s_\infty = 0.65$, $\gamma = 6.45$ pmho, $N = 14{,}000$), in 10 Sr. 100 K−ASW ($I_\infty = -1.64$ nA, $f_c = 12.55$ Hz, $s_\infty = 0.38$, $\gamma = 8.8$ pmho, $N = 5{,}100$), and the system noise at −21 mV. Arrows indicate f_c's. Insets in *B, C, D* show the inactivation in each test *ASW*; ○ shows the control spectrum, and ● shows the test spectrum

membrane in Cs and Ba media (Hagiwara et al., 1976, 1978) and in the frog skeletal muscle fiber in Ba and Sr media (Standen & Stanfield, 1978). In the present analysis, those ions which cause inactivation will be referred to as "inactivators". In addition to those mentioned above, Li^+ is also an inactivator (Ohmori, 1978).

Steady-state current noise, identified as originating from the inactivation process in the anomalous rectifier channels, was analyzed at large negative membrane potentials in Na-ASW (Ohmori, 1978). When the inactivator was changed from 400 mM Na to 10 μM Cs, 50 mM Hydrazine, or 10 mM Sr, the steady-state current noise at a given membrane po-

Table 2. Unitary conductance measured with different kinds of inactivator cations

Inactivator cation		K conc. (mM/liter)	Unitary conductance(γ)[a]	Trial number
Species	Conc.			
Na	400 mM/liter	50	6.56±0.92	167
	210 mM/liter	100	8.37[b]	
Cs	10 μM/liter	100	9.31±0.56	11
Hydrazine	50 mM/liter	50	6.62±0.88	38
Sr	10 mM/liter	100	8.75±0.78	19
	10 mM/liter	50	6.48±1.45	5

[a] γ: mean ± SD.
[b] From Table 2 in Ohmori (1978).

tential changed as shown in Fig. 1. The background noise spectrum (▲) shown in the figure was recorded at zero current potential. In comparison to the control spectrum (at 400 mM Na), the test spectrum (at 10 μM Cs, 50 mM Hydrazine, or 10 mM Sr) shifted clearly to the higher frequency region. Smooth curves were drawn following the Lorentzian formula (Ohmori, 1978).[1]

The analysis of the Lorentzian spectra, as described previously (Ohmori, 1978), shows that the unitary conductance γ, was independent of inactivator species (see Table 2). Experiments were performed either in 50 or in 100 mM K-ASW. The unitary conductance agreed with that in Na-ASW respectively obtained at 50 or 100 mM K in either 400 mM or 210 mM Na-ASW (Table 2). These results indicate that the open state of the channel is not affected by the inactivator species and the inactivation seems to result from an interaction between the open channel and inactivators; each inactivator seems to block the open channels in an all-or-one fashion.

Potential and Concentration Dependence of Inactivation

As already presented in the previous paper (Ohmori, 1978), the inactivation of the K inward current became more marked as the potential became more negative. In this paper the ratio $\Delta I/I_\infty$ (*see* Materials and Methods) was used as the measure of inactivation. It represents the ratio between the number of channels inactivated and the number of channels open in the steady-state. The experimental results show that $\Delta I/I_\infty$ in 50 mM K-ASW changed e-fold with a 19 mV change in membrane potential for Na (Ohmori, 1978), 17 mV for Cs, 27 mV for Hydrazine, and 21 mV for Sr, and that these voltage-dependencies are essentially independent of concentration of inactivators, as clearly shown in Fig. 2 (inset).

The steepness of the blocking as a function of the membrane potential for most inactivators (except Hydrazine and Sr) indicates that the mechanism of inactivation senses more than 100% of the potential across the membrane. It is, therefore, expected that the monovalent inactivators (Na or Cs) inactivate the channel cooperatively either with other cations, which can be the inactivators themselves, or with K ions, or by forming an electric dipole with some gating structure intrinsic to the channel. In order to further characterize these phenomena and define the stoichiometry of binding between the inactivator and the channels, the dependence of blocking on the concentration of the inactivator was determined.

The ratio, $\Delta I/I_\infty$ at a fixed potential was plotted against inactivator concentration on a log-log scale (Fig. 2). Plots approximate a linear line with slope of unity for each inactivator species. This indicates that one inactivator cation binds to one channel in order to inactivate it. Therefore, as a first approximation, the following equation will be appropriate to fit the dependence of blocking on both the concentration of the inactivator and the potential.

$$\Delta I/I_\infty = K_I\,[\text{Inactivator}]_o \exp(-\eta z\psi) \qquad (1)$$

where K_I is an association constant of the inactivator to an affinity site of a channel, η is a constant which can formally interpreted as the fraction of membrane potential that the inactivation mechanism must sense, ψ is FV/RT, and z is the valency of the inactivator. F, R, and T are the usual thermodynamic quantities. η is 1.31 for Na, 1.46 for Cs, 0.92 for Hydrazine, and 0.59 for Sr. The inactivation in Li-ASW was observed only at more negative potential than those at which inactivation is observed in equimolar Na-ASW (Ohmori, 1978), and the inactivation in Ba-ASW was detected at much smaller concentrations of inactivator than in Sr-ASW. Thus, Li is a less potent inactivator than Na, and Ba is a much more potent inactivator than Sr; Ba is the most potent inactivator studied, and Li the least. From Fig. 2 and the equation (1), the potency of inactivation was estimated as follows: Cs > Hydrazine > Na > Li for monovalent inactivators and Ba > Sr for divalent inactivators.

Modulatory Effects upon Inactivation

A clear deviation from linearity is seen for the Na curve of Fig. 2 at concentrations above 100 mM. This

[1] It has not yet been possible to obtain a Lorentzian type noise spectrum in the case of Ba^{2+}, due to the larger time constant of inactivation. In order to estimate a spectrum with statistical confidence similar to that for the other ions, it would be necessary to record for longer periods in steady-state condition, which is not feasible with the present experimental arrangement.

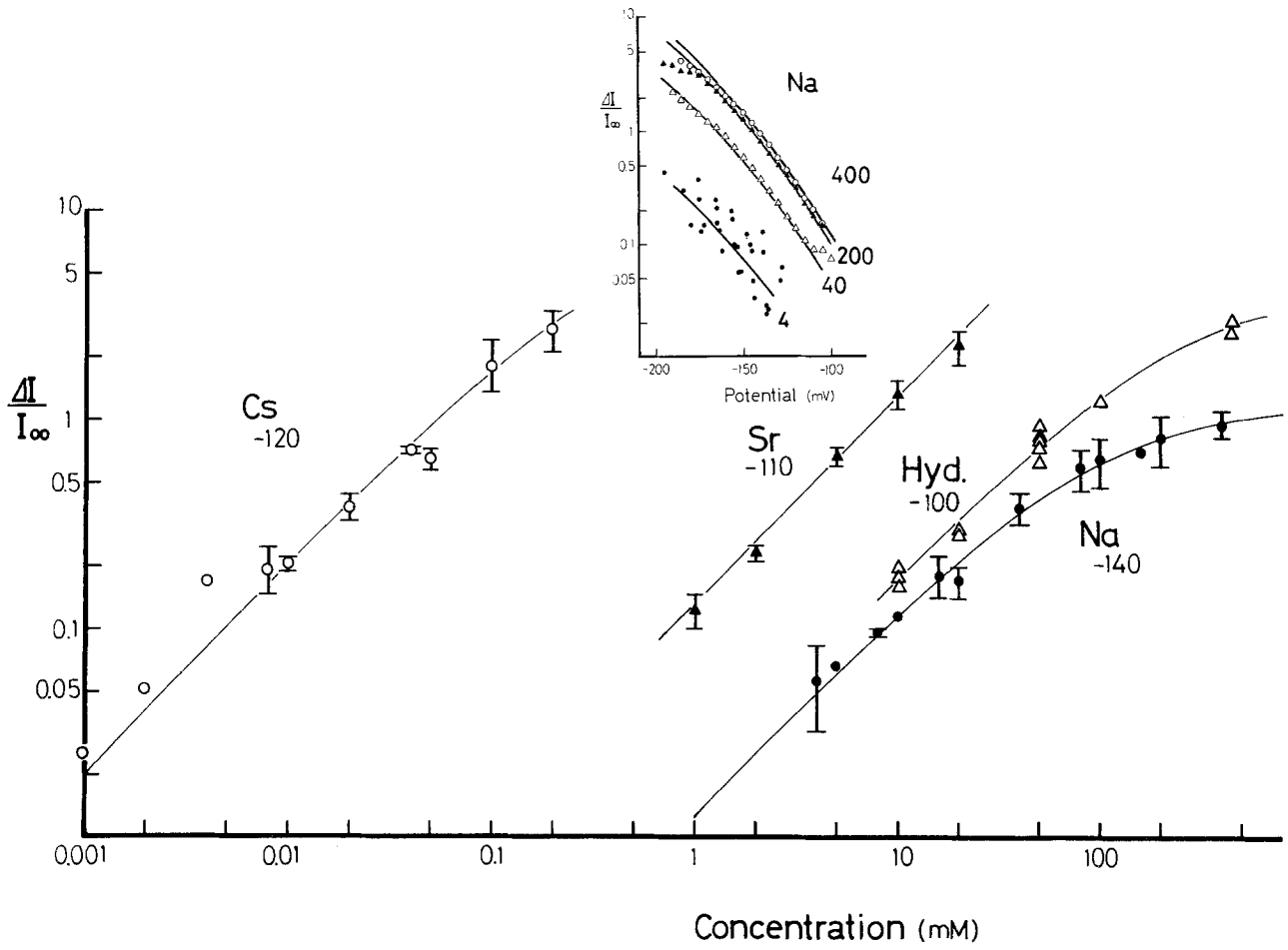

Fig. 2. $\Delta I/I_\infty$ (means and standard deviations) at fixed potentials (indicated in the figure in mV) were plotted against concentration on log-log coordinates in 50 mM K – ASW. The raw data points were plotted for Hydrazine. Insets show the $\Delta I/I_\infty - V$ relation in Na – ASW (●, 4; △, 40; ▲, 200; and ○, 400 mM). The smooth lines were drawn by using Eq. (4) with the parameters presented in Table 3.

saturation is not explained by Eq. (1). The saturation suggests the presence of another binding site within the channel. The state of this site may influence the occupancy of the inactivating site by an inactivator cation. Furthermore, as the slope of $\log(\Delta I/I_\infty)$ against membrane potential was almost independent of the Na concentration within the range from 4 (●) to 400 mM (○) (Fig. 2, inset), this site is likely to be located around the external opening of the channel and to be free from the effects of the membrane potential. Therefore, by simplification, this site can be considered as a special modulatory site located at the external opening of the channel; at least one Na ion must bind to the site to prevent inactivation of the channel. Thus, the experimental formula of the ratio $\Delta I/I_\infty$ will be changed to

$$\Delta I/I_\infty = \frac{K_I' [\text{Inactivator}]_o \exp(-\eta z \psi)}{1 + K_M [\text{Modulator cation}]_o}. \quad (2)$$

Here, K_M is an association constant of modulator cation to the modulatory site, and must be a constant which is independent of the potential. The smooth curves in Fig. 2 were drawn by the inactivation model presented in the Discussion section.

The saturation of $\Delta I/I_\infty$ at higher concentrations was observed not only for Na, but also for Hydrazine and even for Cs (Fig. 2). The slight saturation in Cs or Hydrazine-ASW may also be explained by a presence of some nonspecific leakage current. But the saturation in Na-ASW was larger and the assumption of a nonspecific leakage current was not sufficient to account for the saturation observed. The amount of leakage current was so small (Fig. 3A, 0K) that it caused negligible error in the estimation of $\Delta I/I_\infty$, especially in the potential range more positive than −150 mV. Thus, at least one Na ion must bind to a channel to prevent its inactivation. The binding of a cation to this site probably hinders the entrance of an inactivator into the channel.

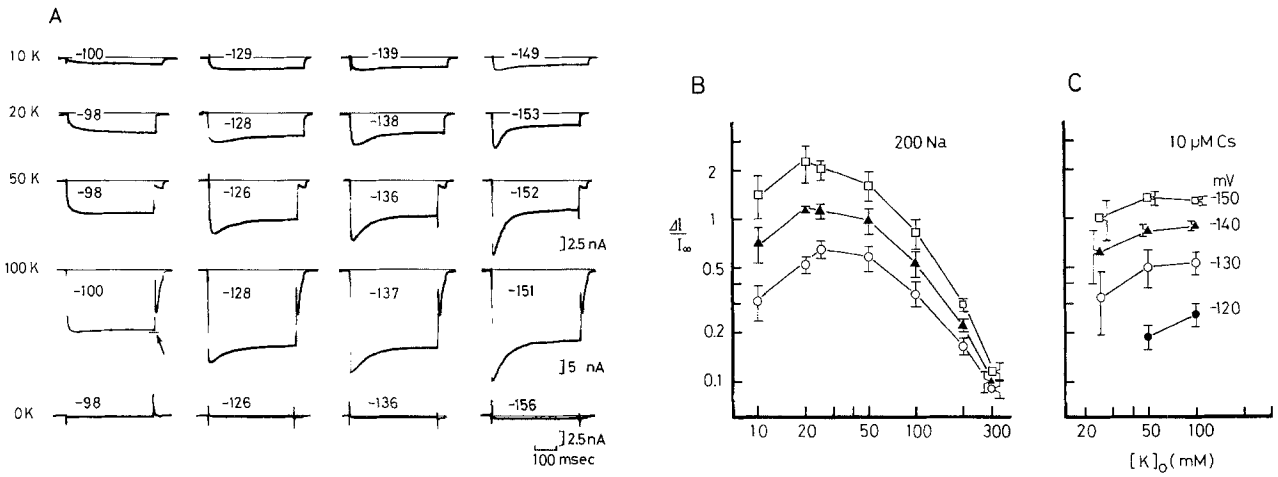

Fig. 3. (*A*): Traces of the inward currents in 10, 20, 50, 100 mM K and in K-free 200 mM Na – ASW. Arrow indicates the level of the peak inward current. (*B–C*): Means and standard deviations of $\Delta I/I_\infty$ at fixed potentials in 200 mM Na – ASW (*B*) and in 10 μM Cs – ASW (*C*) were plotted against $[K]_o$ on log-log coordinates. In *B*, symbols are the same as in *C*

Dual Effects of K Ions upon Inactivation

The results of the above stoichiometric study suggest one-to-one binding of an inactivator to the channel. The potential dependence of inactivation, however, requires that a monovalent inactivator either (1) inactivates the channel cooperatively with some other cation including K^+, or (2) forms an electric dipole with some gating structure intrinsic to the channel. The first possibility was tested by changing the concentrations of ions in ASW other than that of the inactivator. The changes in $[Ca]_o$, $[Mg]_o$, and $[choline]_o$ had no effects upon the inactivation, while, as has been presented in the previous paper (Ohmori, 1978), the inactivation was modified by $[K]_o$.

In 200 mM Na-ASW and for fixed potentials more negative than −130 mV, the extent of inactivation ($\Delta I/I_\infty$) increases with $[K]_o$ at $[K]_o$ lower than 20 mM, while it decreases at $[K]_o$ higher than 25 mM (Fig. 3*A-B*). However, at −100 mV, the inactivation was observed only at 100 mM $[K]_o$ (Fig. 3*A*). The absence of inactivation in 50 mM or lower $[K]_o$ at −100 mV does not seem to be due to the leakage current, because the leakage current is time-independent and negligibly small (Fig. 3*A*, 0K). Clearly, only the activation was observed at −100 mV at 10 or 20 mM $[K]_o$. Extracellular K ions do indeed seem to increase the extent of inactivation at −100 mV. Therefore, the inactivation is not only a function of membrane potential but also a function of $[K]_o$. K ions seem to increase (facilitate) the inactivation on the one hand and decrease (suppress) it on the other hand, depending upon the concentration and the membrane potential.

Quantitative Interpretation of the Facilitatory Effects of K Ions upon the Inactivation

In order to determine the facilitatory effects of $[K]_o$ upon the inactivation, $\Delta I/I_\infty$ values at several potentials were plotted against $[K]_o$ on a log-log graph (Fig. 3*B*, 200 mM Na-ASW; 3*C*, 10 μM Cs-ASW). The slopes of the graph changed from positive ($[K]_o < 20$ mM) to negative ($[K]_o > 25$ mM) and became increasingly more negative as $[K]_o$ increased in 200 mM Na-ASW. The positive slopes were close to one and were almost independent of the membrane potential, but the negative slopes became steeper as the membrane potential became more negative (Fig. 3*B*). This observation strongly suggests that one K ion inactivates the channel cooperatively with an Na ion. The facilitatory action of K ions upon inactivation becomes obscured as $[K]_o$ increases because of the stronger suppressive effects of the same K ions upon inactivation.

The positive relation between $\Delta I/I_\infty$ and $[K]_o$ was also observed in 10 μM Cs-ASW, in which case the slope decreased as the membrane potential became more negative, and at −150 mV, a portion of the negative slope was finally observed (Fig. 3*C*). A similar facilitation of inactivation by K ions in Cs-ASW has been reported by Hagiwara et al. (1976) for the anomalous rectifier of the starfish egg membrane. The inactivation caused by Sr showed no facilitation by K ions (Fig. 5*B*). Since Sr is a divalent cation, the steepness of the inactivation against membrane potential can be explained by a simple divalent-cation-

channel interaction mechanism (Hagiwara et al., 1978; Standen & Stanfield, 1978).

Quantitative Interpretation of the Suppressive Effects of K Ions upon the Inactivation

As clearly shown in Fig. 3*A–B* the suppression of the inactivation by extracellular K ions is more potent than the facilitation in Na-ASW. This suppression of the inactivation by extracellular K ions is not only manifested by the shift of the inactivation-potential relation to more negative potentials, but also by a change in the steepness of the membrane potential dependence of inactivation; the membrane potential dependence of inactivation changed from 15 mV at 10 mM $[K]_o$ to 30 mV at 100 mM $[K]_o$ for an *e*-fold change of $\Delta I/I_\infty$ (estimated from Fig. 3*A*). Therefore, either K_I' is a function of both $[K]_o$ and membrane potential, or η is a function of $[K]_o$ in Eq. (2). However, since η is generally interpreted as the location of the inactivating site within a channel (at least when $\eta<1$), it is reasonable to postulate that this quantity is independent of $[K]_o$.

Since the positive slope of the relation between $\log(\Delta I/I_\infty)$ and $\log [K]_o$ is about one (Fig. 3*B*), it is assumed that one K ion inactivates the channel cooperatively with one Na ion. The suppressing K ions probably are K ions within an open channel; they perhaps suppress inactivation by preventing the inactivator from occupying the inactivating site within the channel, which should be reflected in the decrease of K_I'. Therefore, K_I' in Eq. (2) must be transformed to a function which has a numerator proportional to $[K]_o$ and a denominator consisting of a power series of $[K]_o$. Therefore, the ratio $\Delta I/I_\infty$ would be expressed as follows:

$$\begin{aligned}\Delta I/I_\infty &= \frac{K_I''[\mathrm{In}]\exp(+\eta z\psi)}{1+K_M[M]_0} \cdot \frac{[\mathrm{HK}]_o}{a_0+a_1[\mathrm{K}]_o+a_2[\mathrm{K}]_o^2+\ldots+a_j[\mathrm{K}]_o^j+\ldots} \\ &= \frac{K_I''[\mathrm{In}]\exp(-\eta z\psi)}{1+K_M[M]_0} \cdot \frac{1}{(a_0/[\mathrm{K}]_o+a_1+a_2[\mathrm{K}]_o+\ldots a_j[\mathrm{K}]_o^{j-1}+\ldots)}.\end{aligned} \quad (3)$$

Here, K_I'' and a_j's are constants at a fixed potential and j is the number of suppressive K ions within an open channel with probability proportional to a_j at the steady state.

The measurement of $\Delta I/I_\infty$ at a fixed potential in various K concentrations would reveal the number of suppressive K ions within an open channel with highest probability. Fig. 3*B* suggests (1) that the terms at least from a_0 to a_2 are dominant for $[K]_o$ less than 100 mM, and the higher order terms become dominant as $[K]_o$ increases; (2) and that there is little effect of membrane potential upon the slope at $[K]_o$ lower than 20 mM, but at $[K]_o$ higher than 50 mM the negative slope becomes steeper as the potential becomes more negative. These results indicate that about two K ions are present within an open channel and act suppressively to the inactivation in Na-ASW at $[K]_o$ smaller than 100 mM, and the number of K ions within an open channel increases not only due to the increase of $[K]_o$, but also due to the membrane hyperpolarization.

The above observation may be explained by assuming that there is a series of binding sites within a channel. If K ions bind sequentially to the successive sites during transport, the above observation suggests that the probability of the binding of more than one K ion simultaneously to several sites within a channel is affected by $[K]_o$ as well as by the membrane potential. Both hyperpolarization and the increase of $[K]_o$ enhance the probability of the binding of multiple K ions within an open channel.

Discussion

The present experimental results suggest that both monovalent and divalent inactivator cations bind in a one-to-one stoichiometry to the K anomalous rectifier channel of the egg cell membrane of the tunicate (Fig. 2). However, the steepness of the membrane potential dependence of inactivation caused by monovalent inactivators (Na or Cs) is not entirely consistent with this stoichiometric relation (Fig. 2). The difficulty was qualitatively resolved by invoking the facilitatory effects of the extracellular K ions upon inactivation (Fig. 3). Namely one extracellular K ion would inactivate the channel cooperatively with an Na^+ or a Cs^+, while two extracellular K ions would suppress the same inactivation, especially at high $[K]_o$ or at large negative membrane potential.

There may be at least two possible explanations for the gating mechanism of the inactivation observed above. One is to assume an inherent gating molecule in the channel, similar to that considered originally in the activation and inactivation gates of the Na-channel (Hodgkin & Huxley, 1952). By association with one inactivator cation the molecule may form an electric-dipole, which may be stabilized by the further association with facilitatory K^+. A similar mechanism has been proposed by Hagiwara et al., (1977) for the activation of anomalous rectifier. The other is the inactivation caused by a plugging of the inactivator into a channel, a mechanism suggested by

Armstrong for the inactivation of the delayed-K-channel by TEA-derivatives (Armstrong, 1971, 1975).

Both mechanisms seem to explain the experimental results described above. In the Na or Ca channels, because the difference in the species of permeating cations does not modify the time course of the ionic currents nor the steepness of the membrane potential dependence of the gating kinetics, gating functions are considered to be more likely achieved by inherent structural parts of the channel than by the movement through or binding to the channel of freely diffusible ions (Frankenhaeuser & Hodgkin, 1957; Hagiwara & Naka, 1964; Chandler & Meves, 1965; Hille, 1971, 1972; Okamoto et al., 1976; Ohmori & Yoshii, 1977). However, in the anomalous rectifier studied in this paper, the variation in $[K]_o$ resulted in the modification of the kinetics of the inactivation of the K-inward currents (Fig. 3), which consisted not only of a simple shift of the gating mechanism against the membrane potential but also of a change in the steepness of the membrane potential dependence of the inactivation mechanism itself. Since these results are quite suggestive of multiple occupancy of K ions within an open channel, the second type of approach is considered below to account for the experimental results in the following discussions.

The concept of multiple-sites permeation has already been proposed by Hodgkin and Keynes (1955) as the mechanism of *single-file* diffusion in the K channel. The results presented in this paper seem to be an example of the single-file diffusion of K ions through the anomalous rectifier. Recently, Hille and Schwarz (1978) reviewed and calculated extensively the mechanism of multiple-site permeation.

The possible existence of at least two serially located binding sites within an open channel in standard 50 mM K-ASW (Fig. 3) is consistent with the cooperative inactivation of a monovalent inactivator with a K ion. The inactivated state caused by the entrance of only one monovalent inactivator into the channel is probably an intermediate and unstable state (subgroup-*I*) and will promptly change into other states, i.e., into the open state (subgroup-*O*) by the backward jump of the inactivator cation from the channel or into the stably inactivated state (subgroup-*C*) by the further occupation of the outer site by a K ion. Probably, once an inactivator has entered the channel, it is unable to retract due to the K ion following behind. The reaction rate of inactivation, then, may be determined mainly by the second process, occupation of outer site by a K ion. By this cooperative inactivation, the steepness of the potential dependence of steady-state inactivation, (namely a value for $\eta > 1$) can be explained even for a monovalent inactivator cation (Ciani, Hagiwara & Miyazaki, 1977).

The hypothetical energy profiles within channel at zero applied potential are presented for a permeating K ion (Fig. 4 *A-a*), for a monovalent inactivator (solid line), and for a plugging K ion (broken line) (Fig. 4*A-b*), with the nomenclature used in the following discussion. If the ionic transport through the channel follows a mechanism of vacant site occupation and not a knock-on mechanism, the diagram of states-transitions derived from Fig. 4*A* would be the one presented in Fig. 4*B*, in which each subgroup is enclosed by a broken line. The rate constants k_{ij} (for K^+) and n_{ij} (for monovalent inactivator) are for the transition from site i to j with the potential dependence prescribed by Eyring rate theory. α, β, and γ represent the fraction of electrical distances between the sites. These electrical distances and the energy profile could be changed for different ionic species. Therefore, the electrical locations of the binding sites would be different for inactivated states (α', β', γ', Fig. 4*A-b*) than they are for the open states (α, β, γ, Fig. 4*A-a*), probably reflecting the differences in ionic size and in electrostatic potential energies between ionic species.

For simplification, the rate constants of K ion to pass over the innermost energy barrier (G_{34}) are assumed to be much smaller than the other rate constant for a K ion. Thus, the transitions between S_0 and S_2, S_1 and S_3 would be negligible. If it is further assumed that the rate constants across the energy barrier G_{02} is the largest, S_2 in subgroup-*O* would promptly change to S_3, and the steady-state probability of S_2 would become negligible. Particularly in the transition from S_4 to S_5, if the outward movement of K ions across the barrier (G_{34}) is further assumed negligible because of the electrostatic repulsive force due to the already existing inactivator cation within the channel, the steady-state conditional probability of S_5 in subgroup-*I* would also be negligible, and the transitions between S_2 and S_5 and then between S_4 and S_5 would be negligible. These assumptions considerably simplify the states-transitions-diagram (to only the transitions indicated by solid arrows in Fig. 4*B*). The subgroup-*I* itself would be negligible, because the monovalent inactivators inactivate the channel only cooperatively with K ions (Fig. 3). In addition, the presence of a modulatory site is assumed [Eq. (2) and (A9)].

The steady-state open probability of the channel (s) was determined by the diagrammatic method (King & Altman, 1956; Hill, 1966; Chizmadjev & Aityan, 1977; Hille & Schwarz, 1978) under the assumptions made above (*see* Appendix). Given the potential en-

ergy of a cation at each site relative to that in external solution, Eq. (A10) becomes

$$\Delta I/I_\infty = \frac{\frac{[In^+]}{1+[M]e^{-U_1}}[K]_o e^{-U_3-G_3'}e^{-(2\alpha'+\beta')\psi}}{1+[K]_o e^{-G_2}e^{-\alpha\psi}+[K]_o^2 e^{-G_2-G_3}e^{-(2\alpha+\beta)\psi}}. \quad (4)$$

Equation (4) is equivalent to the experimentally-derived formula (3) in every respects. The time constant of inactivation (τ_s) (A8) is calculated from a second order differential equation for s (A6), as follows:

$$\tau_s = s_\infty/k_{20}^*. \quad (5)$$

Curves were fitted by changing one parameter at a time to get the best fit to the experimental points by eye. At first, the K^+ binding sites (α, β) in the open states were assumed both to be 0.3, and then the parameters for Na-mediated inactivation in the steady-state ($\Delta I/I_\infty$) were determined. U_1's were estimated from the stoichiometric relations in Fig. 2, considering the inactivator also to be the modulator cation. The parameters for the other inactivators which mediate inactivation were then determined by the same procedure, keeping the open state parameters, α' and β' unchanged as much as possible. For Sr^{2+}, the curve was fitted assuming S_4 is a stably inactivated state and that Sr^{2+} has quite low affinity to the modulatory site (site-1). In this case, subgroup-*C* was neglected. Finally, the parameters for the time constants were determined; k_{20}^* was chosen to fit the curves to the data points obtained with highest inactivator concentration for each species. The parameters determined are listed in Table 3. Small changes in open-state parameters, α' and β', might reflect cellular differences and the contribution of leakage current. The downward deviation of the experimental results from the exponential dependence on membrane potential was fitted to some extent by the simulated curves (Fig. 2, inset, and Fig. 5*A*). The remaining systematic deviation of the experimental points from the calculated curves in these figures might be caused by the leakage current which becomes prominent at highly hyperpolarized potentials. If prompt inactivation with the time constant τ_1 occurred (*see* A7), it could also cause such deviations.

When $[K]_o$ was changed between 25 and 100 mM, the data for steady-state inactivation by Na and Cs (Fig. 5*C–D*) were fitted well with the parameters determined already, with slight modifications (Table 3). Sr ions showed no obvious interaction with K ions (Fig. 5*B*). However, the bendings at large negative potential seem to indicate the presence of suppressive effects of extracellular K ions upon inactivation caused by Sr^{2+}.

Time constants were also calculated using Eq. (5) with parameters already determined and k_{20}^* (Fig. 6*A–D*, broken lines). Except for Na, the calculated curves fit well. Even for Na, slight modification of the value U_1 determined in Fig. 2 would cause the simulated curves to fit better. The effects of saturation upon the time constants are not so large as are those upon steady-state inactivation. This discrepancy might reflect the simplified treatment of the modulatory site (*see* Appendix). $[K]_o$-dependent change of τ_s (Fig. 6*E–F* for Na and Cs) were also fitted well by the same set of parameters as determined in Fig. 5. K^+ shows a facilitatory interaction with Sr^{2+} in the time constants (Fig. 6*G*), which is contrary to the observation in $\Delta I/I_\infty$ (Fig. 5*B*).

The two-binding-site (with one modulatory site) model presented here can explain the experimental results, not only qualitatively but to some extent quantitatively. But this simplified model fails in several points, especially in the inactivation caused by Sr ions. Also the time-constant-potential relations were not fitted satisfactorily. These failures seem to reflect the simplifications of the model, because the real permeation and the channel blocking processes may consist of several steps more, and the mechanism of knock-on permeation may also be included, especially for the inactivation caused by Sr ions.

One of the experimental results which cannot be explained by this model is the Na-concentration-dependent change of the chord conductance; chord conductance in Na-free ASW is much smaller than that in Na-ASW (Ohmori, 1978). The results of noise analysis (Table 4) indicated that this increase is due to the increase in number of channels as $[Na]_o$ increases and is not due to the changes in the unitary conductance. This may result from some facilitatory effect of Na ions upon the anomalous rectifier (Ohmori, 1978). In recent experiments involving internal perfusion of the starfish egg, a small amount of intracellular Na ions is found necessary to activate ionic currents through the anomalous rectifier (Hagiwara & Yoshii, 1979). In terms of a model which recently has been formulated by Ciani et al. (1978), the formation of open channels requires the presence of 'gating ion'. It may very well be, then, that Na^+, although impermeant, plays double roles of 'inactivator' and 'gating ion', so that the overall conductance of anomalous rectifier to K^+ may be determined by the competition of these two effects.

Appendix

This appendix contains brief derivations of the equations used in the *Discussion* section. In the following

derivations, only the transitions between the states connected by solid arrows (Fig. 4*B*) were considered. The several assumptions made in order to simplify the transitions-diagram were described in the *Discussion* section.

Suppose the k_{ij}'s in Fig. 4 much larger than the n_{ij}'s, except for the state transition between S_6 and S_7, which must be influenced by the inactivator within the channel and may be considered as the rate-limiting step. Thus, the total channel states would be divided into three subgroups, each in quasi-equilibrium; *O*pen, *I*ntermediate and *C*losed. Both *I* and *C* are closed subgroups.

If the probabilities that each channel is in subgroup-*O*, -*I* and -*C* are expressed as s, s_I and s_C, respectively, the set of equations characterizing the random process would be as follows.

$$s+s_I+s_C=1 \tag{A1}$$

$$\frac{ds}{dt}=s_I(\theta_4+\theta_5)n_{20}-s(\theta_0+\theta_2)n_{02} \tag{A2}$$

$$\frac{ds_C}{dt}=s_I\theta_6 k^*_{02}-s_C k^*_{20}. \tag{A3}$$

Here, θ_i's mean the steady-state conditional probability of each state-i (S_i in Fig. 4*B*) within each quasi-equilibrated subgroup, i.e., $\theta_0+\theta_1+\theta_2+\theta_3=1$, $\theta_4+\theta_5+\theta_6=1$. The θ-values were determined by diagrammatic methods. Since the steady-state probability s_I and the probabilities θ_2 and θ_5 are considered negligible, the steady-state open probability of a channel, s, simplifies to

$$s(=s_\infty)=\frac{1}{1+\dfrac{\theta_0 n_{02}}{\theta_4 n_{20}}\theta_6\dfrac{k^*_{02}}{k^*_{20}}}. \tag{A4}$$

The ratio $\Delta I/I_\infty$ in the steady-state is then,

$$\Delta I/I_\infty=\frac{\dfrac{n_{02}n_{23}k^*_{02}}{n_{20}n_{32}k^*_{20}}}{1+\dfrac{k_{02}}{k_{20}}+\dfrac{k_{02}k_{02}k_{23}}{k_{20}k_{20}k_{32}}}. \tag{A5}$$

Both the numerator and denominator of Eq. (A5) are exponential functions of membrane potential, and it is possible to explain the steep potential dependence of $\Delta I/I_\infty$ by determining the affinities of each site to K and to the inactivator, and the electrical distances between the sites ($\alpha, \alpha', \beta, \beta'$).

In order to estimate the kinetic property of the model, a second order differential equation for s is derived from Eq. (A1)–(A3) as follows.

$$\frac{d^2s}{dt}+(\theta_6 k^*_{02}+k^*_{20}+(\theta_4+\theta_5)n_{20}+(\theta_0+\theta_2)n_{02})\frac{ds}{dt}$$
$$+((\theta_0+\theta_2)n_{02}\theta_6 k^*_{02}+(\theta_4+\theta_5)n_{20}k^*_{20}$$
$$+(\theta_0+\theta_2)n_{02}k^*_{20})s$$
$$=(\theta_4+\theta_5)n_{20}k^*_{20}. \tag{A6}$$

If Eq. (A6) is solved under the assumptions made above, $n_{02}+n_{20}\gg k^*_{02}+k^*_{20}$, θ_2 and $\theta_5\ll 1$, and $s_I\ll 1$, the time constants of inactivation are

$$\tau_1=1/[\theta_0 n_{02}+\theta_4 n_{20}] \tag{A7}$$

and

$$\tau_s\simeq 1/[1+\Delta I/I_\infty]k^*_{20}=s_\infty/k^*_{20}. \tag{A8}$$

Qualitatively, Eq. (A8) satisfies the observations; τ_s changes in parallel with s_∞ (Ohmori, 1978). The inactivation caused by the smaller time constant τ_1 is insignificant because the steady-state probability s_I is assumed to be negligible. Therefore, the time constant τ_2 is considered equal to the time constant of inactivation, τ_s. k^*_{20} is affected by the inactivator cation within the channel and could be different from one inactivator species to another. k^*_{20} determines the absolute value of τ_s.

Equations (A5) and (A8) can explain steep potential dependence of the inactivation and the almost parallel change of s_∞ and τ_s with membrane potential and inactivator concentrations (Figs. 5–6). However, to explain the saturation observed in Fig. 2, especially for Na, a new site must be added, a membrane potential independent modulatory site (site-1). This site must have high affinity for the modulator, and occupation of this site by a modulator cation would not allow the channel to be inactivated. Therefore, this site is probably located in the rather large external mouth of the channel; so the hydrated K ions can pass by the modulator bound to site-1, but the hydrated inactivators (especially Na) would be incapable of passing by, mainly because of the steric restriction. By the introduction of this modulatory site-1, the model becomes effectively a three-site, four-barrier one. However, if the association and dissociation of a modulator cation with this site-1 are not only independent of K transport through the channel, but also are very fast, and if the occupation of site-1 by a modulator cation does not interfere with the exit of an inactivator from the channel (the transition from S_4 to S_0), the treatment of this three-site model is simplified. The only modification from the former model is to change the rate constant n_{02} to

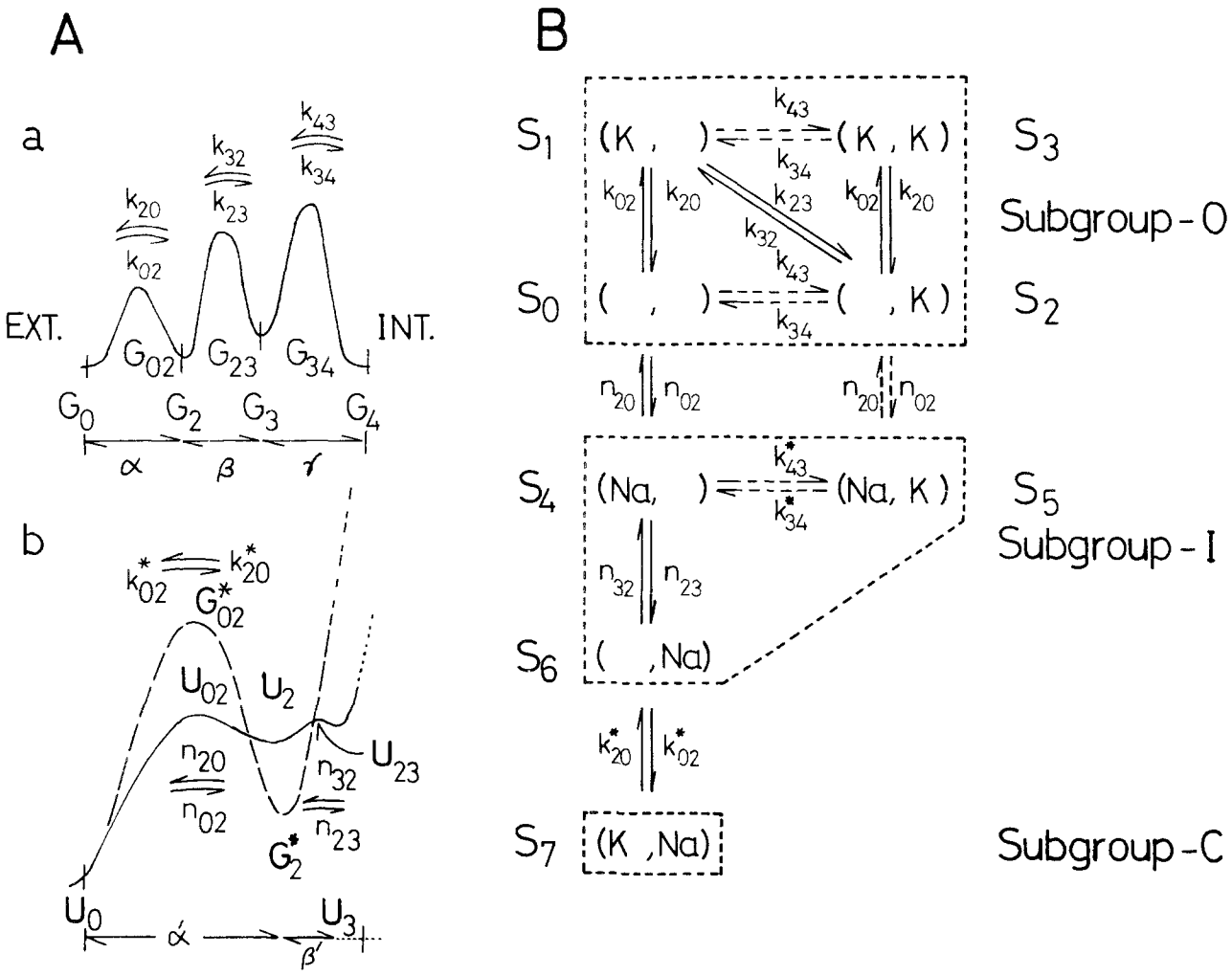

Fig. 4. Diagrams of the hypothetical energy profiles of a permeating K ion (*Aa*) and an impermeating inactivator (solid line) and a plugging K ion (broken line), (*Ab*) within a channel, and the basic diagram of the states-transitions (*B*). (*A*): Two binding sites (2 and 3) are assumed within a channel with chemical potential energy, G_2 and G_3 for K, and U_2 and U_3 for an inactivator. k_{ij}'s and n_{ij}'s are rate constants for transitions of a permeating K ion and an impermeating inactivator from site i to site j with electrical potential dependence prescribed by Eyring rate theory. α, (α'), β, (β'), and γ are electrical distances between each site. (*B*): Channel states are indicated in parentheses: (site-2, site-3). In this diagram, Na was used to represent the monovalent inactivator

Table 3. Parameters of the gating model

Open states					Closed states						Remarks
Type	α	β	G_2	G_2+G_3	α'	β'	U_1	$U_3+G_2{}^*$	$k^*{}_{20}{}^a$		
									$\delta\alpha'$	$Q\exp(-G^*{}_{02}+G_2{}^*)$	
Na	0.3	0.3	−0.1	−1.1	0.7	0.2	−2.33	2.59	0.05	0.014	Figs. 2, 6*A*
Na-K	0.3	0.3	−0.1	−1.1	0.7	0.2	−2.33	2.48	0.05	0.014	Figs. 5*C*, 6*E*
Cs	0.3	0.3	2	−0.5	0.75	0.2	−7.61	−4.97	0.35	0.5	Figs. 2, 5*A*, 6*B*
Cs-K	0.3	0.3	3	0.5	0.75	0.2	−7.61	−4.97	0.35	0.66	Figs. 5*D*, 6*F*
Hyd.	0.3	0.3	0	−3	0.6	0.2	−1.38	−1.33	0	0.064	Figs. 2, 5*A*, 6*C*
Sr	0.3	0.3	1	−1.5	0.7	–	–	$U_2=0.82$	0.02	0.025	Figs. 2, 5*A*, 6*D*

[a] $k^*{}_{20}=Q\exp(-G^*{}_{02}+G^*{}_2)\exp(-\delta\alpha'\psi)$; Q is a frequency factor in msec^{-1}. G_i's and U_i's are in RT units.

Except for U_1's, parameters were determined by fitting the curves to the experimental points by eye. U_1's were determined by least-squares fits from $I_\infty/\Delta I-1/[\mathrm{In}^+]$ diagrams. The parameters are defined in Fig. 4. Details in text.

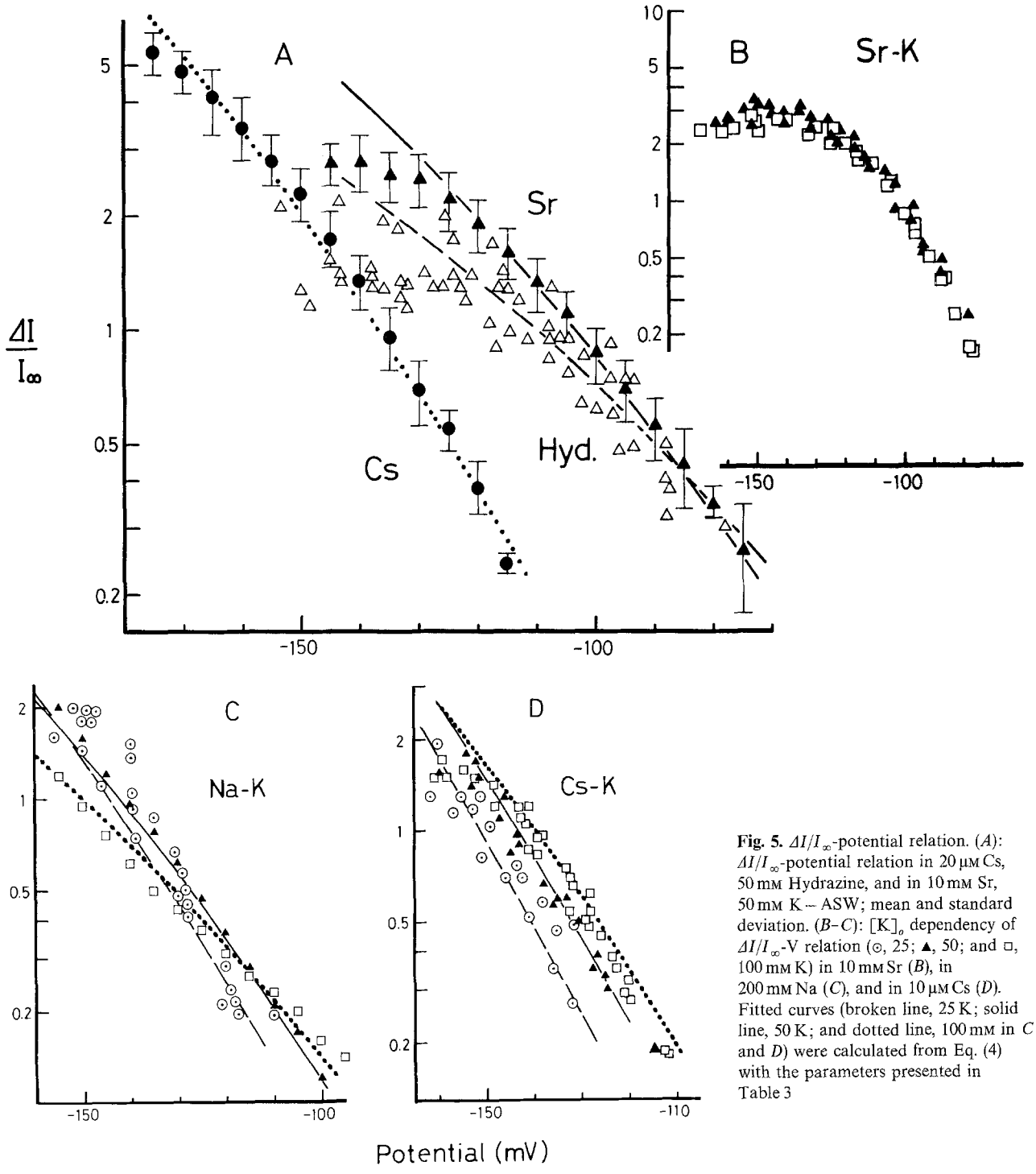

Fig. 5. $\Delta I/I_\infty$-potential relation. (*A*): $\Delta I/I_\infty$-potential relation in 20 μM Cs, 50 mM Hydrazine, and in 10 mM Sr, 50 mM K – ASW; mean and standard deviation. (*B–C*): $[K]_o$ dependency of $\Delta I/I_\infty$-V relation (⊙, 25; ▲, 50; and □, 100 mM K) in 10 mM Sr (*B*), in 200 mM Na (*C*), and in 10 μM Cs (*D*). Fitted curves (broken line, 25 K; solid line, 50 K; and dotted line, 100 mM in *C* and *D*) were calculated from Eq. (4) with the parameters presented in Table 3

$$\frac{n_{02}}{1+[M]\frac{m_{01}}{m_{10}}}. \tag{A9}$$

Here, m_{01} and m_{10} are potentially independent, and the ratio m_{01}/m_{10} is the chemical affinity of modulator cation to the site-1. Therefore, Eq. (A5) will be modified to

$$\Delta I/I_\infty = \frac{\dfrac{1}{1+[M]\dfrac{m_{01}}{m_{10}}}\cdot\dfrac{n_{02}n_{23}k^*_{02}}{n_{20}n_{32}k^*_{20}}}{1+\dfrac{k_{02}}{k_{20}}+\dfrac{k_{02}k_{02}k_{23}}{k_{20}k_{20}k_{32}}}. \tag{A10}$$

The steady-state properties of inactivation would also be explained if the subgroup-*I* consisted only of

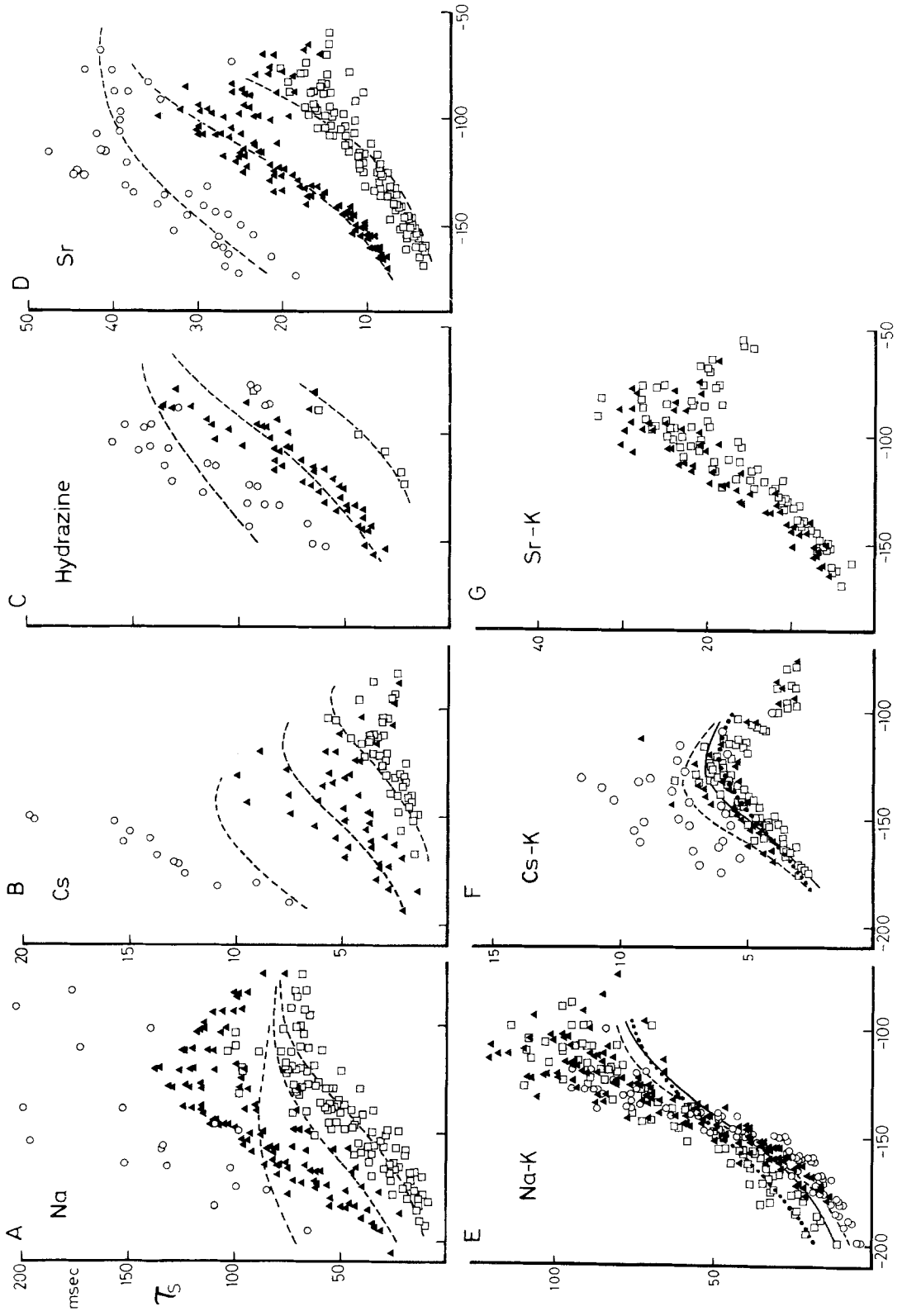

Fig. 6. Time constants of inactivation. (*A*): In 4 (○), 40 (▲), and 400 mM Na (□); 50 mM K ASW. (*B*): In 5 (○), 20 (▲), and in 100 μM Cs (□); 50 mM K ASW. (*C*): In 10 (○), 50 (▲), and in 450 mM Hydrazine (□); 50 mM K ASW. (*D*): In 1 (○), 5 (▲), and in 20 mM Sr (□); 50 mM K ASW. (*E–G*): $[K]_o$ (○, 25; ▲, 50; □, 100 mM) dependent τ_s changes in 200 mM Na (*E*), 10 μM Cs (*F*), and in 10 mM Sr ASW (*G*). Fitted curves (broken line, 25 K; solid line, 50 K; dotted line, 100 mM K) were calculated from Eq. (5) with the parameters presented in Table 3.

Table 4. Effects of $[Na]_o$ upon γ and N

Cell name	Na conc (mM/liter)	$\bar{g}_K$ [a] ($\times 10^{-8}$ mho)	N [b] (per egg)	γ [b] (pmho)	Trial no.
50	400	3.23	5474± 635	6.50±0.62	10
	50	2.91	3581± 276	6.33±0.6	2
	80	3.13	4626	6.05	1
108	400	5.54	7993±1168	6.52±0.76	6
	100	3.63	5690± 871	6.30±0.7	5
110	400	6.12	5695±1169	6.72±0.91	4
	200	3.24	4243± 303	6.82±0.43	3
111	200	5.63	6760±1153	7.22±0.66	2
	400	7.58	7886± 385	7.06±0.58	4
113A	400	4.84	6369± 456	6.74±0.21	6
	200	3.19	5181± 715	6.44±0.83	4
114A	400	5.52	8280± 695	6.74±0.46	8
	200	4.61	6840± 333	6.82±0.3	2
114	200	1.83	3926±1557	6.58±1.85	2
	400	4.90	5537± 552	7.38±0.66	3
116	200	2.22	3166± 494	6.71±0.7	2
	400	3.58	4742± 182	6.64±0.21	4
121	300	4.29	5927± 246	6.23±0.17	7
	400	4.91	7003± 884	6.64±0.5	6

[a] $\bar{g}_K$: maximum chord conductance obtained from relaxational voltage-clamp run.
[b] N, γ: mean ± SD.

S_4 and S_5, and if S_6 were included in stably inactivated subgroup-*C*. In this case, however, the membrane potential dependence of τ_s becomes less steep than that predicted by Eq. (A8). Even equation (A8) fails to explain the steep membrane potential dependence of τ_s in some cases.

It is my pleasure to express my acknowledgement to Dr. K. Takahashi for his valuable advice and discussions at all stages of this work. I thank Professor S. Hagiwara, Professor A. Takeuchi, Dr. S. Ciani, and Dr. W. L. Byerly for their many valuable criticisms of the manuscript. Financial support from the Japan Society for the Promotion of Science as a predoctoral fellow is gratefully acknowledged.

References

Armstrong, C.M. 1971. Interaction of tetraethylammonium ion derivative with the potassium channel of giant axons. *J. Gen. Physiol.* **58**:413

Armstrong, C.M. 1975. K pores of nerve and muscle membrane. *In:* Membranes. Vol. 3, p. 325. G. Eisenman, editor. Marcel Dekker, New York

Bendat, J.S., Piersol, A.G. 1971. Random Data: Analysis and Measurement Procedures. Wiley Interscience, New York

Chandler, W.K., Meves, H. 1965. Voltage clamp experiments on internally perfused giant axons. *J. Physiol. (London)* **180**:788

Chizmadjev, Yu. A., Aityan, Kh.S. 1977. Ion transport across sodium channels in biological membranes. *J. Theor. Biol.* **64**:429

Ciani, S., Hagiwara, S., Miyazaki, S. 1977. A model for Cs blocking of the K conductance in anomalous rectification. *Biophys. J.* **17**:46*a*

Ciani, S., Krasne, S., Miyazaki, S., Hagiwara, S. 1978. A model for anomalous rectification: Electrochemical-potential-dependent gating of membrane channels. *J. Membrane Biol.* **44**:103

Frankenhaeuser, B., Hodgkin, A.L. 1957. The action of calcium on the electrical properties of squid axons. *J. Physiol. (London)* **137**:218

Gay, L.A., Stanfield, P.R. 1977. Cs^+ causes a voltage-dependent block of inward K currents in resting skeletal muscle fibres. *Nature (London)* **267**:169

Hagiwara, S., Miyazaki, S., Krasne, S., Ciani, S. 1977. Anomalous permeabilities of the egg cell membrane of a starfish in $K^+ - Tl^+$ mixtures. *J. Gen. Physiol.* **70**:269

Hagiwara, S., Miyazaki, S., Moody, W., Patlak, J. 1978. Blocking effects of barium and hydrogen ions on the potassium current during anomalous rectification in the starfish egg. *J. Physiol. (London)* **279**:167

Hagiwara, S., Miyazaki, S., Rosenthal, N.P. 1976. Potassium current and the effect of cesium on this current during anomalous rectification of the egg cell membrane of a starfish. *J. Gen. Physiol.* **67**:621

Hagiwara, S., Naka, K. 1964. The initiation of spike potential in barnacle muscle fibres under low intracellular Ca^{2+}. *J. Gen. Physiol.* **48**:141

Hagiwara, S., Yoshii, M. 1979. Effects of internal K and Na on the anomalous rectification of the starfish egg as examined by the internal perfusion. *J. Physiol. (London) (in press)*

Hill, T.L. 1966. Studies in irreversible thermodynamics. IV. Diagrammatic representation of steady state fluxes for unimolecular systems. *J. Theor. Biol.* **10**:442

Hille, B. 1971. The permeability of the sodium channel to organic cations in myelinated nerve. *J. Gen. Physiol.* **58**:599

Hille, B. 1972. The permeability of the sodium channel to metal cations in myelinated nerve. *J. Gen. Physiol.* **59**:637

Hille, B., Schwarz, W. 1978. Potassium channels as multi-ion single-file pores. *J. Gen. Physiol.* **72**:409

Hodgkin, A.L., Huxley, A.F. 1952. A quantitative description of membrane current and its application to conduction and excitation in nerve. *J. Physiol. (London)* **117**:500

Hodgkin, A.L., Keynes, R.D. 1955. The potassium permeability of a giant nerve fibre. *J. Physiol. (London)* **128**:61

Keynes, R.D., Rojas, E. 1976. The temporal and steady-state relationship between activation of the sodium conductance and movement of the gating particles in the squid giant axon. *J. Physiol. (London)* **255**:157

King, E.L., Altman, C. 1956. A schematic method of deriving the rate laws for enzyme-catalyzed reactions. *J. Phys. Chem.* **60**:1375

Ohmori, H. 1978. Inactivation kinetics and steady state current noise in the anomalous rectifier of tunicate egg cell membranes. *J. Physiol. (London)* **281**:77

Ohmori, H, Yoshii, M. 1977. Surface potential reflected in both gating and permeation mechanisms of sodium and calcium channels of the tunicate egg cell membrane. *J. Physiol. (London)* **267**:429

Okamoto, H., Takahashi, K., Yoshii, M. 1976. Membrane currents of the tunicate egg under the voltage-clamp condition. *J. Physiol. (London)* **254**:607

Standen, N.B., Stanfield, P.R. 1978. A potential- and time-dependent blockade of inward rectification in frog skeletal muscle fibres by barium and strontium ions. *J. Physiol. (London)* **280**:169

Received 15 October 1979